International Journal of Heat and Mass Transfer 52 (2009) 3079–3083

Contents lists available at ScienceDirect

International Journal of Heat and Mass Transfer

journal homepage: www.elsevier.com/locate/ijhmt

Flow separation in a diverging conical duct: Effect of Reynolds number and divergence angle

E.M. Sparrow [a], J.P. Abraham [b,*], W.J. Minkowycz [c]

[a] Laboratory for Heat Transfer and Fluid Flow Practice, Department of Mechanical Engineering, University of Minnesota, Minneapolis, MN 55455-0111, USA
[b] Laboratory for Heat Transfer and Fluid Flow Practice, School of Engineering, University of St. Thomas, St. Paul, MN 55105-1079, USA
[c] University of Illinois at Chicago, Department of Mechanical and Industrial Engineering, Chicago, IL 60607-7022, USA

ARTICLE INFO

Article history:
Received 3 January 2009
Received in revised form 9 February 2009
Accepted 9 February 2009
Available online 26 March 2009

Keywords:
Flow separation
Diffuser
Cross-sectional enlargement
Laminarization
Flow transitions

ABSTRACT

Fluid flows in passages whose cross-sectional area increases in the streamwise direction are prone to separation. Here, the flow in a conical diffuser fed by a fully developed velocity at its inlet and mated at its downstream end to a long circular pipe is investigated by means of numerical simulation. A universal flow-regime model was used to accommodate possible laminarization of flows having moderate-turbulent and transitional Reynolds numbers at the diffuser inlet. It was found that flow separation occurred for a diffuser expansion angle of 5° for inlet Reynolds numbers less than about 2000. This finding invalidates a prior rule-of-thumb that flow separation first occurs at a divergence angle of seven degrees. Results from the 10 and 30° simulations showed separation at all investigated Reynolds numbers. The largest streamwise length of the separation zones occurred at the lower Reynolds numbers.

1. Introduction

The knowledge base for the design of piping systems and heat exchange installations must include information on the occurrence of flow separation in fittings and valves. This is because flow separation is a major cause of pressure drop and also impacts the magnitude of heat transfer coefficients.

Flows in passages whose cross-sectional area increases in the streamwise direction are recognized as being vulnerable to separation. In the literature relevant to such flows, there exists a rule of thumb for the effect of the divergence angle of the passage on the potential for flow separation. In particular, for diverging conical passages, the rule states that for total angles of divergence less than seven degrees, separation will not occur. For larger divergence angles, separation is to be expected [1]. Another source states that "angles greater than 15 degrees cause flow separation" [2]. Both the 7- and the 15-degree recommendations are mute about the possible effect of the Reynolds number. The uncertainties of how flow separation depends on both the divergence angle and the Reynolds number are of practical importance and motivate the present work.

From a literature review, it appears that the present state of knowledge is largely based on experiments reported by Gibson [3] in 1910. These experiments, when carefully scrutinized, appear to be flawed with respect to the goal of the study. In particular, the results are based on pressure differences between a station slightly upstream of the diffuser inlet and a second station situated in a pipe attached to the exit end of the diffuser. The information obtained encompasses flow phenomena that occur not only in the diffuser proper but also in the downstream straight pipe. In that downstream pipe, the flow is by no means the same as that which would occur under fully developed conditions since the flow exiting the diverging section carries with it a legacy. In the respected fluid-flow textbook by White [2], curves depicting the pressure loss in the diverging passage are provided and are attributed to Gibson's data [3]. One of the ambiguities of that information is that it is not indicated whether the presented pressure drop is that in the diffuser proper or whether it includes additional downstream pressure losses associated with the redevelopment of the flow in the straight pipe. The Gibson data are also used as the basis of recommended pressure drop information for diverging conical ducts in the oft-quoted handbook published by Crane [4].

Another much-cited source of pressure drop data for a variety of fittings, valves, and other obstructions is the compendium due to Fried and Idelchik [1]. The experimental methods on which the cited information is based are not described. Furthermore, it is unclear whether the quoted pressure drop information applies to the diverging passage proper or expresses the overall pressure drop which occurs not only in the diverging passage but also in the downstream pipe where redevelopment occurs.

It is also noteworthy that all of the prior work cited in the preceding paragraphs pertains to Reynolds numbers of 50,000 and

* Corresponding author. Tel.: +1 651 962 5766; fax: +1 651 962 6419.
E-mail address: jpabraham@stthomas.edu (J.P. Abraham).

0017-9310/$ - see front matter © 2009 Elsevier Ltd. All rights reserved.
doi:10.1016/j.ijheatmasstransfer.2009.02.010

Nomenclature

a	SST model constant
d	upstream diameter
D	downstream diameter
E	turbulence destruction terms
F_1, F_2	blending functions in SST model
k	turbulence kinetic energy
$\dot{m}$	mass flowrate
P	model production term
Re	Reynolds numbers, $4\dot{m}/\mu\pi d$ or $4\dot{m}/\mu\pi D$
S	absolute value of the shear strain rate
u	velocity
x	streamwise coordinate
x_i	tensor coordinate

Symbols

α	SST model constant
β_1, β_2	SST model constants
ω	specific rate of turbulence dissipation
μ	dynamic viscosity
θ	total angle of divergence
Π	intermittency adjunct function
γ	intermittency
ρ	density
σ	diffusion parameters

Subscripts

i,j	tensor indices
t	turbulent

higher. In most of the work, no particular attention was given to Reynolds-number effects.

The approach to be implemented here is to use numerical simulation to definitively explore the fluid mechanics of conical diverging passages. To the best knowledge of the authors, such an investigation has not previously been attempted, especially when the plethora of possible flow regimes is taken into consideration. When fluid flows in a diverging passage, its Reynolds number decreases in the direction of fluid flow. If the flow entering the passage were to be in the moderate-Reynolds-number turbulent regime, there is a possibility that it may undergo a transition to an intermittent flow or to a laminar flow. This process may be termed laminarization. Fluid-flow models that are capable of dealing with flow transitions and which are self predicting have not heretofore been available for internal flows. Very recently, the present authors have developed such a model. This model enables the flowing fluid to experience the proper flow regime. Without this feature, it is highly unlikely that accurate solutions for flows in diverging passages could be obtained.

The scope of the present investigation encompasses passages with total divergence angles of 5, 10, and 30 degrees. For each divergence, the values of the Reynolds number at the inlet of the diverging passage are varied between 500 and 33,000.

The results of the study will be reported by means of numerically created flow visualizations.

2. Model

A schematic diagram of the situation that is simulated here is shown in Fig. 1. A fully developed flow is delivered to the inlet cross section of the conical diffuser. The diffuser provides a transition between a pipe of diameter d and a larger downstream pipe whose diameter is D. The diffuser total angle is θ. The action of the diffuser is to decrease the initial Reynolds number by a factor of d/D. If the flow entering the diffuser is laminar, there is no change in flow regime as the fluid passes through the enlarging cross section. On the other hand, a turbulent flow passing through the diffuser may experience a change of flow regime (laminarization). That evolution of flow regime may cause the flow at the diffuser exit to be either intermittent or laminar. Depending on the size of the angle of divergence and the magnitude of the diffuser-inlet Reynolds number, the flow passing through the diffuser may not be able to follow the contour of the bounding walls. This occurrence, commonly termed *flow separation*, may give rise to pressure losses and may also disrupt expected rates of heat transfer in thermal applications. The exit of the diffuser is attached to a circular pipe which is of sufficient length to enable the flow to become fully developed.

In the past, in order to implement the numerical simulation, two different fluid-mechanic models would have had to be used to accommodate the cases of laminar or turbulent inlet flow. For the laminar case, the governing equations encompass mass conservation and the full Navier–Stokes equations. In the case of a turbulent flow at inlet, a much more complex mathematical description is necessary. In contrast, the numerical simulation is implemented here by making use of a universal flow-regime model which is capable of automatically predicting the appropriate flow regime and providing the proper solution for the self-selected regime.

The present approach requires the consideration of three sets of interlocking equations: (a) momentum and mass conservation for turbulent flow, (b) turbulence model (Shear Stress Transport), and (c) transitional flow model.

The first of the sets encompasses the equation of continuity and the RANS equations, which are

$$\frac{\partial u_i}{\partial x_i} = 0 \tag{1}$$

$$\rho\left(u_i \frac{\partial u_j}{\partial x_i}\right) = -\frac{\partial p}{\partial x_j} + \frac{\partial}{\partial x_i}\left((\mu + \mu_t)\frac{\partial u_j}{\partial x_i}\right) \quad j = 1,2,3 \tag{2}$$

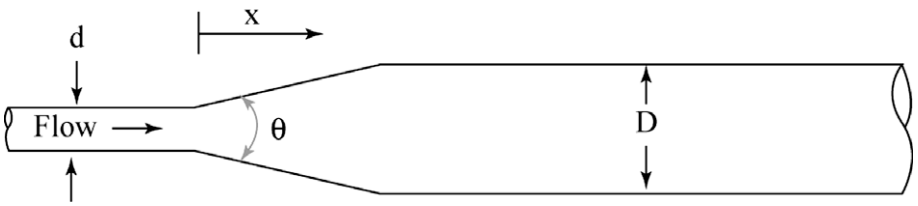

Fig. 1. Schematic model of the simulation geometry.

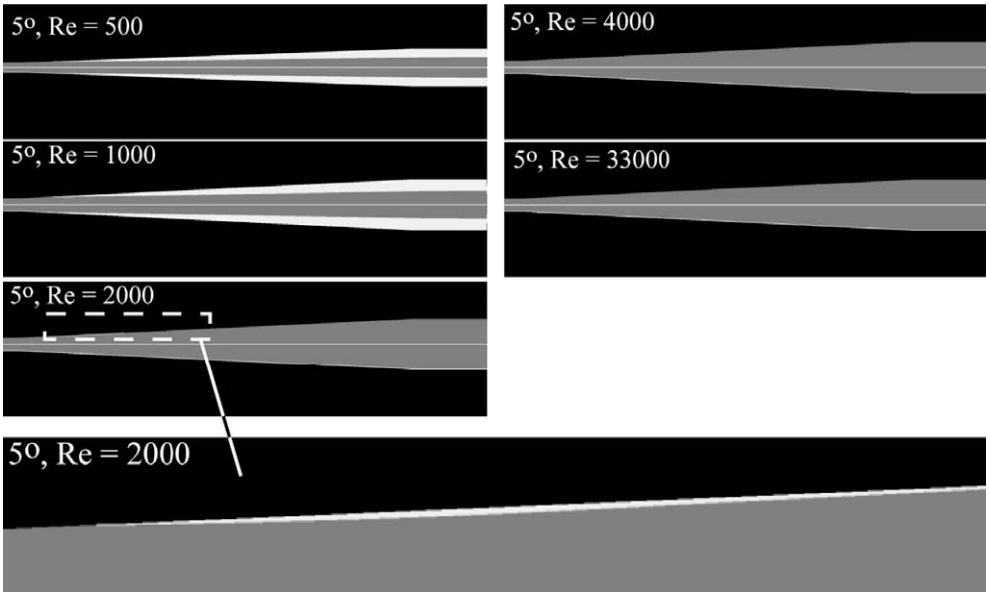

Fig. 2. Flow visualization patterns within the 5° diffuser and in the adjacent downstream pipe.

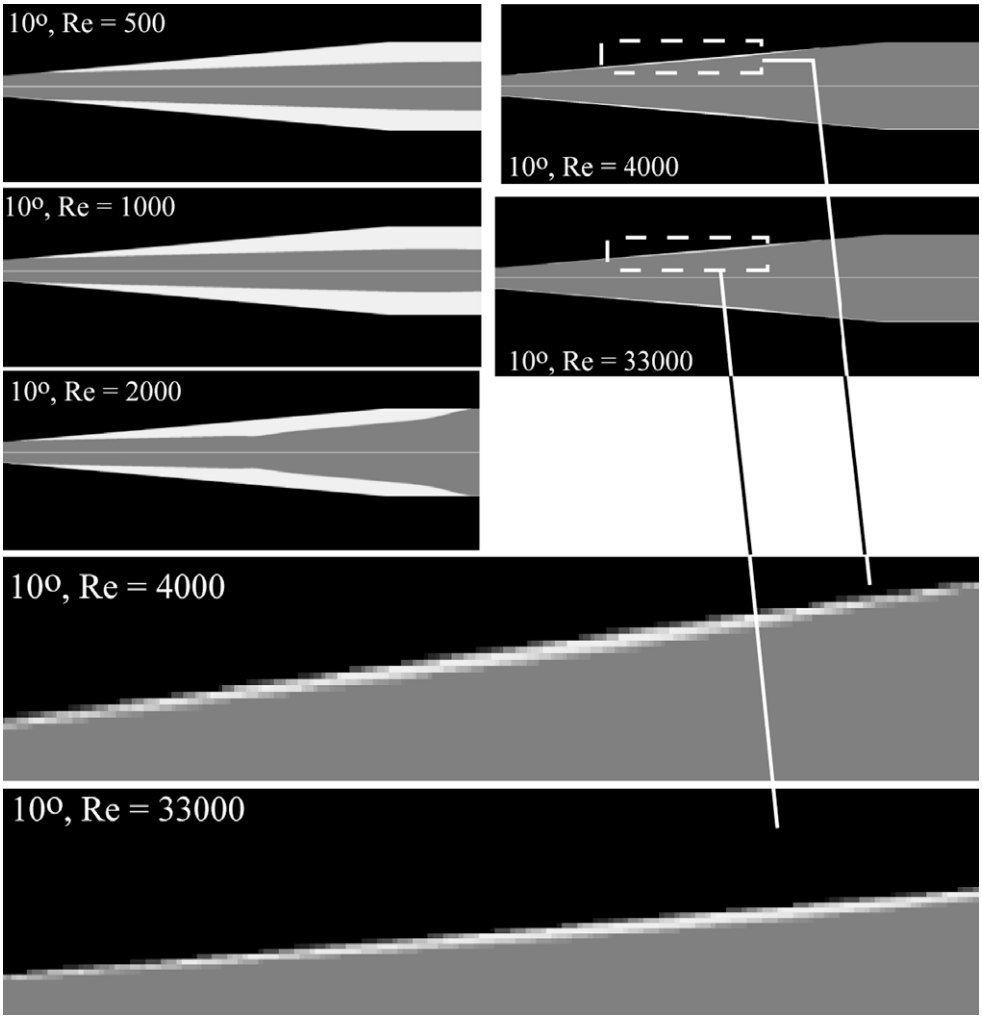

Fig. 3. Flow visualization patterns within the 10° diffuser and in the adjacent downstream pipe.

Here, μ_t is the so-called turbulent viscosity. To obtain values of this quantity, it is necessary to make use of a supplementary pair of equations.

The chosen turbulence model from which μ_t is extracted is the so-called Shear Stress Transport Model (SST) [5]. The choice of this model is based not only on its proven competence in dealing with internal flows but also because it is linked to a newly devised model of flow-regime transition. The dependent variables of the SST model are the turbulence kinetic energy k and the specific rate of turbulence destruction ω. The governing equations for these quantities are

$$\frac{\partial(\rho u_i k)}{\partial x_i} = \gamma P_k - \beta_1 \rho k\omega + \frac{\partial}{\partial x_i}\left[\left(\mu + \frac{\mu_t}{\sigma_k}\right)\frac{\partial k}{\partial x_i}\right] \tag{3}$$

and

$$\frac{\partial(\rho u_i \omega)}{\partial x_i} = \alpha\rho S^2 - \beta_2 \rho\omega^2 + \frac{\partial}{\partial x_i}\left[\left(\mu + \frac{\mu_t}{\sigma\,_{\omega 1}}\right)\frac{\partial \omega}{\partial x_i}\right] + 2(1 - F_1)\rho\frac{1}{\sigma_{\omega 2}\omega}\frac{\partial k}{\partial x_i}\frac{\partial \omega}{\partial x_i} \tag{4}$$

The solution of Eqs. 3 and 4 yields the turbulent viscosity μ_t in terms of k and ω by means of

$$\mu_t = \frac{a\rho k}{\max(a\omega, SF_2)} \tag{5}$$

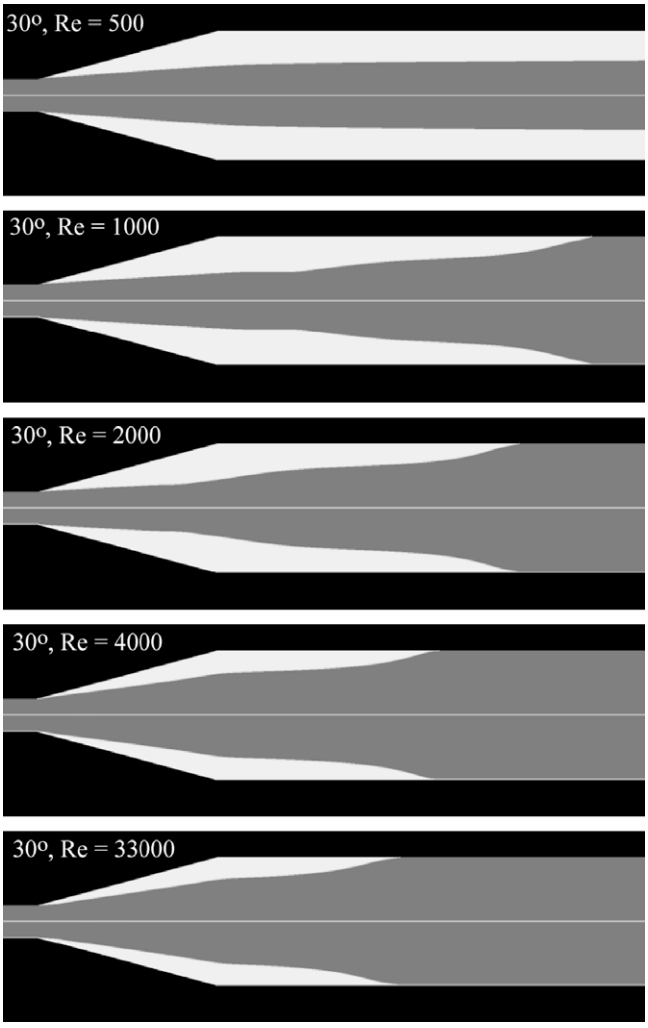

Fig. 4. Flow visualization patterns within the 30° diffuser and in the adjacent downstream pipe.

in which F_2 is a blending function that limits the turbulent viscosity within the boundary layer. Equation 3 is, in fact, a modification of the original version of the SST model in that it contains a multiplying factor γ, termed the intermittency, which acts on the turbulence production term P_k. In the conventional form of the SST model, the factor 1 appears in lieu of γ. It is the role of γ to diminish the production term in regions of turbulent intermittency. Further details of the SST model can be found in [6].

The equation used for the prediction of γ is [6–8].

$$\frac{\partial(\rho u_i \gamma)}{\partial x_i} = P_{\gamma,1} - E_{\gamma,1} + P_{\gamma,2} - E_{\gamma,2} + \frac{\partial}{\partial x_i}\left[\left(\mu + \frac{\mu_t}{\sigma_\gamma}\right)\frac{\partial \gamma}{\partial x_i}\right] \tag{6}$$

Embedded in the turbulent production and destruction terms, P and E, respectively, is the quantity Π which may be designated as the turbulent adjunct function. The governing equation for Π is

$$\frac{\partial(\rho u_i \Pi)}{\partial x_i} = P_{\Pi,t} + \frac{\partial}{\partial x_i}\left[\sigma_{\Pi,t}(\mu + \mu_t)\frac{\partial \Pi}{\partial x_i}\right] \tag{7}$$

The mathematical statement of the problem is embodied in the eight equations, Eqs. (1)–(4), (6), and 7, where Eq. (2) encompasses three equations. These equations are strongly coupled and must be solved simultaneously.

2.1. Numerical implementation

To implement the numerical simulation, use was made of CFX version 11.0 software.

The number of nodes used to obtain acceptable, mesh-independent solutions was 430,000. Validation of the numerical solutions was obtained by comparing the values of fully developed friction factors in the pipe downstream of the diffuser with available correlations of experimental data. In all cases, agreement to within 1% or better was achieved. In addition, care was taken to achieve residuals of 10^{-6} or smaller for all variables, except for the intermittency residual which was typically 10^{-5}.

Boundary conditions for the numerical simulation include the no-slip and impermeability conditions on all solid boundaries. At the inlet of the diffuser, a fully developed velocity profile, either laminar or turbulent, depending on the situation under consideration, was imposed. At the downstream end of the solution domain, the streamwise second derivatives of the velocities were required to be zero and a reference pressure was specified.

3. Results and discussion

The main results of the numerical simulation are displayed by means of numerically created flow visualizations and are presented in Figs. 2–4, respectively for divergence angles of 5, 10, and 30 degrees. Each figure is a collage of separate panels, with each panel corresponding to a specific diffuser-inlet Reynolds number ranging from 500 to 33,000. In each panel, the diffuser geometry is outlined against a black background. When appropriate, a portion of the downstream pipe is also included in the outlined geometry. To aid in the interpretation of the displayed results, note that the gray zones denote regions of forward flow, and the zones of solid white are the back-flow regions. The very thin white lines demarking the outboard edges of the outlined geometry are not to be confused with the separated regions.

Attention may first be turned to Fig. 2 to view the results for the 5° divergence case. It is clear that separated regions are in evidence for diffuser-inlet Reynolds numbers of 500 and 1000. At first glance, it would appear that separation has disappeared for $Re = 2000$. However, a magnification of the visualization panel for this Reynolds number, shown at the bottom of the figure, reveals the continued existence of separation. The visualization panels

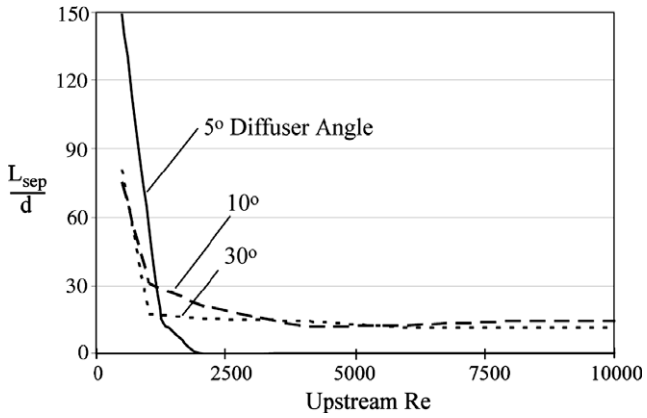

Fig. 5. Dependence of the length L_{sep} of the separation region on the diffuser-inlet Reynolds number.

for Re = 4000 and 33000, no matter at what magnification, do not display separated regions. It may, therefore, be concluded that flow separation can occur for divergence angles of 5° for $Re \leq 2000$. This outcome invalidates both the seven- and 15-degree thresholds for separation set forth in [1,2] respectively.

Focus is next directed to the results for the 10° divergence (Fig. 3). At the lower Reynolds numbers, 500, 1000, and 2000, the separated region not only spans the full length of the diffuser but also penetrates into the pipe downstream of the diffuser. The extent of the downstream penetration increases with decreasing Reynolds numbers. At the higher Reynolds numbers, 4000 and 33,000, magnification is used to demonstrate that flow separation continues to exist, but it is confined to the diffuser proper.

Fig. 4 is for the 30° diffuser angle. For this case, there is a robust separated region filling the diffuser and extending downstream for all of the investigated Reynolds numbers. The downstream penetration of the zone of separation diminishes as the Reynolds number increases.

To provide quantitative information for the streamwise length L_{sep} of the separated region, Fig. 5 has been prepared. That figure shows the dependence of L_{sep}/d on the diffuser-inlet Reynolds number. For all three diffuser angles, lower values of the Reynolds number give rise to longer separated regions. With increasing Reynolds number, the separation zones decrease in extent. The figure shows that L_{sep}/d is very sensitive to the Reynolds number for $Re < 2000$ but is insensitive at larger values of Re. For the 5° diffuser angle, the separated region disappears at $Re \sim 2000$. For the larger diffuser angles (10 and 30°), the length of the separation region reaches a minimum value which is independent of further increases in the Reynolds number. To provide perspective for these results, it may be noted that the axial lengths of the three diffusers are 34.2d, 22.9d, and 11.5d, respectively for the 5, 10, and 30° cases.

Finally, it should be noted that the model correctly predicted relaminarization for those cases whose downstream Reynolds numbers were in the laminar range, as assessed by the fully developed friction factor.

4. Concluding remarks

The method of numerical simulation has been employed here to provide definitive information about flow separation in conical diffusers. The published literature contains conflicting information about the effect of the diffuser divergence angle on the onset of separation and is altogether silent about the effect of the Reynolds number. Flows entering the diffuser at moderate-turbulent and transitional Reynolds numbers may experience a laminarization process. A universal flow-regime model was used here to accommodate this behavior.

The specific physical situation chosen for study here is a conical diffuser which receives a fully developed flow at its inlet and mates with a long circular pipe at its exit. The downstream pipe is long enough to allow full development of the flow. Simulations were performed for total angles of divergence of 5, 10, and 30°. For each divergence angle, the Reynolds number at the diffuser inlet was varied from 500 to 33,000. The ratio of the diffuser exit-end diameter to its inlet-end diameter was fixed at four for these studies.

For a divergence angle of 5°, flow separation was found to occur for diffuser-inlet Reynolds numbers less than approximately 2000. This finding invalidates a previous assertion that separation-free operation would occur for divergence angles less than seven degrees. A second prior assertion suggested that separation would not occur until the divergence angle reached 15°. For diffuser angles of 10 and 30°, the simulations showed that separation occurred for all of the investigated diffuser-inlet Reynolds numbers.

Another goal of the work was to identify the streamwise length of the separated region. For all the investigated diffuser angles, the longest separated regions occurred at the lowest values of the diffuser-inlet Reynolds number. With increasing Reynolds numbers, the length of the separated region diminished.

As already noted, the separated region for the 5° diffuser disappeared altogether for $Re \sim 2000$. For the 10 and 30° divergence cases, the length of the separated region became insensitive to the Reynolds number at higher Re. For most of the investigated cases, the separated region extended downstream from the diffuser exit into the downstream pipe.

Acknowledgements

Support of H. Birali Runesha and the Supercomputing Institute for Digital Simulation & Advanced Computation at the University of Minnesota is gratefully acknowledged.

References

[1] E. Fried, I.E. Idelchik, Flow Resistance: A Design Guide for Engineers, Hemisphere Publishing Corporation, New York, 1989.
[2] F.M. White, Fluid Mechanics, sixth ed., McGraw Hill, Berlin, 2008.
[3] A.H. Gibson, On the flow of water through pipes and passages having converging or diverging boundaries, Proc. Roy. Soc. A 83 (1920) 366–378.
[4] Anon., Flow of fluids through valves, fittings and pipe technical paper no. 410m, Crane Valves, The Woodlands, TX, 1999.
[5] F.R. Menter, Two-equation eddy-viscosity turbulence models for engineering applications, AIAA J. 32 (1994) 1598–1605.
[6] F.R. Menter, T. Esch, S. Kubacki, Transition modelling based on local variables, in: 5th International Symposium on Engineering Turbulence Modeling and Measurements, Mallorca, Spain, 2002.
[7] F.R. Menter, R.B. Langtry, S.R. Likki, Y.B. Suzen. P.G. Huang, S. Volker, A correlation-based transition model using local variables, Part I – model formulation, in: Proceedings of ASME Turbo Expo Power for Land, Sea, and Air, Vienna, Austria, June 14–17, 2004.
[8] F.R. Menter, R.B. Langtry, S.R. Likki, Y.B. Suzen. P.G. Huang, S. Volker, A correlation-based transition model using local variables, Part II – test cases and industrial applications, in: Proceedings of ASME Turbo Expo Power for Land, Sea, and Air, Vienna, Austria, June 14–17, 2004.